

- Earthquake Engrg., Vol. 3, No. 4, pp 495–518, 1999.
- [11] Priestly MJN, Kowalsky MJ, Ranzo G, Benzoni G., Preliminary development of direct DBD for MDOF systems, Proc. of the 65th Annual Convention, SEAOC, Maui, Hawaii, 1996.
 - [12] Calvi G.M. & Pavese A., DBD of building structures, European seismic design practice, Belkema, Rotterdam, 1995.
 - [13] Medhekar M.S. & Kennedy D.J.L., Displacement seismic design of buildings- Theory, Int. Jour. of Engrg. Structures, Vol.22, pp201-209, 2000.
 - [14] Medhekar M.S. & Kennedy D.J.L., Displacement seismic design of buildings- Application, Int. Jour. of Engrg. Structures, Vol.22, pp210-221, 2000.
 - [15] Chandler A.M. & Mendis P.A., Performance of RC frames using force and displacement seismic assessment methods, Int. Jour. of Engrg. Structures, Vol.22, 2000.
 - [16] Chandler AM, Tsangaris M., Lam NTK, Wilson JL, Edwards M., Hutchinson GL., Seismic performance of RC structures using displacement based principles, 11ECEE, Balkema, Rotterdam, 1998.
 - [17] M.Tehranizadeh, M.Safi and S.A. Alavinasab, Calculation of design spectra for Iran using intelligent classification of earthquake records, Submitted to JSEE.
 - [18] European Seismic Standard, EC8, 1994.
 - [19] Krawinkler H, Seneviratna GDPK., Pros and cons of a Pushover Analysis of seismic performance evaluation, Engrg. Struct., Vol.20, No.(4-6), pp452–464, 1998.
 - [20] Paz M., Dynamic of structures, Mc Graw Hill inc., 1996.
 - [21] SAP2000, Structural Analysis Program, Computers & Structures Inc., California, USA, 1999.
 - [22] Kannan AE, Powell GH., Drain-2D: a general-purpose computer program for dynamic analysis of inelastic plane structures, Report no. EERC 73-6, Univ. of California, Berkeley, California, 1973.
 - [23] Miranda E., Bertero V.V., Evaluation of strength reduction factors, Earthquake Spectra, Vol. 10, No. 2, pp 357-379, 1994.
 - [24] Chandler AM, Lam NTK, PBD in earthquake engineering: a multidisciplinary review, Engrg. Struct., Vol.23, pp1525–1543, 2001.
 - [25] Rosenblueth E, Herrera I., On a kind of hysteretic damping, Journal of Engineering Mechanics Division ASCE, Vol.90, pp37– 48, 1964.
 - [26] Paulay T., A simple displacement compatibility based seismic design strategy for RC buildings, 12WCEE, New Zealand, 2000.
 - [27] Paulay T., DBD approach to earthquake induced torsion in ductile buildings, Eng. Struct., Vol.19, No.9, pp699–707, 1997.
 - [28] Prestandard for Seismic Rehabilitation of Buildings, Federal Emergency Management Agency, FEMA356, 2000.

m_i	Story mass
M_p	Plastic section moment
P_u	Compressive strength of column
T_{eff}	Effective period
V_b	Base shear
V_i	Story shear
V_{iy}	Story yield shear
Z	Plastic section modulus
α	Strain hardening ratio
δ_{ci}	Story displacement due to column deformation
δ_{eff}	Effective displacement
δ_i	Story displacement
δ_{yi}	Story yield lateral displacement
Δ	Roof lateral displacement
μ	Global ductility
μ_i	Story ductility
μ_r	Reduced ductility
θ_{dd}	Distortional drift
θ_p	Plastic joint rotation
σ_y	Yield stress
ξ_{eff}	Effective damping ratio
$\xi_{elastic}$	Elastic damping ratio

References

- [1] Fajfar P. Capacity spectrum method based on inelastic demand spectra. *Earthquake Engrg. Struct. Dynamics*, pp Vol. 28, No. 9, pp 79–93, 1999.
- [2] Chopra AK, Goel RK. Capacity-demand-diagram methods for estimating seismic deformation of inelastic structures: SDOF systems, Report No. PEER-1999-02, Univ. of California, Berkeley, 1999.
- [3] Freeman SA. Development and use of capacity spectrum method, Proceedings of the 6th US National Conf. on Earthquake Engrg., Seattle, EERI, Oakland, California, 1998.
- [4] Fajfar P., A nonlinear analysis method for performance based seismic design, *Earthquake spectra*, Vol. 16, No. 3, pp 573-592, 2000.
- [5] Fajfar P., Equivalent ductility factors taking into account low-cycle fatigue, *Earthquake Eng. Struct. Dynamics*, Vol. 21, No. 9, pp 837–848, 1992
- [6] Shibata A, Sozen MA. Substitute-structure method for seismic design in RCs, *Journal of the Structural Division ASCE*, Vol. 102, pp 1-18, 1976.
- [7] Kowalsky MJ, Priestley MJN, MacRae GA., DBD, a methodology for seismic design applied to SDOF RC structures, Report No. SSRP-94/16, Univ. of California, San Diego, La Jolla, California, 1994.
- [8] Calvi GM, Kingsley GR., Displacement-based seismic design of MDOF bridge structures, *Earthquake Engrg. Struct. Dynamics*, Vol. 24, No. 9, pp1247–1266, 1995.
- [9] Qi X, Moehle JP. Displacement design approach for RC structures subjected to earthquakes, Report No. UCB/EERC-91/02. Berkeley, University of California, 1991.
- [10] Panagiotakos TB, Fardis MN. Deformation-controlled earthquake-resistant design of RC buildings, J.

calculated. As shown the obtained periods may vary up to 150 percent.

- As expected the ductility demand in eccentric systems had the highest values having other specifications constant. This ductility was highly dependent to the plastic rotations in the mid length link beams. It has also been shown that the lateral story force has not been so sensitive to the ductility pattern but the displacement and drift directly change with the ductility. The effective damping, total base shear, mass and effective height ratio which may be assumed as the representative for lateral force distribution are not sensitive to the ductility distribution over height and just depend on the maximum ductility value.
- Although greater value of damping results in a greater effective period in the displacement spectrum and thus less base shear for the design, this study confirmed that neglecting of the effect of damping in the use of elastic response spectrum will result in a conservative design.
- As the relationship between member strains or member plastic rotations with the inter-story drifts are determined, both local and global performance criteria may be used for such a design method.

As shown by various examples, various effects such as column deformation effects, torsional effects, higher mode effects, $P - \Delta$ effects and low cycle fatigue effects may easily be assessed by the use of equivalent procedures in the direct DBD.

Acknowledgment

The supports by the department of research and development of the Paymabargh Power Engineering Contractor Company are gratefully acknowledged.

Notations

Symbol	Definition
A	Gross sectional area of beam or column
A_b	Brace sectional area
a_{eff}	Effective acceleration
a_i	Story acceleration
E	Elasticity modulus
E_s	Second modulus
f_i	Story force
f_{yi}	Story yield force
H	Total height of the building
H_{eff}	Effective height of the building
H_f	Height of applying lateral building force
H_i	Story height
K_{eff}	Effective stiffness
K_p	Plastic section stiffness
L	Total building width
L_b	Brace length
L_l	Link beam length
L_s	Braced panel span
m_{eff}	Effective mass

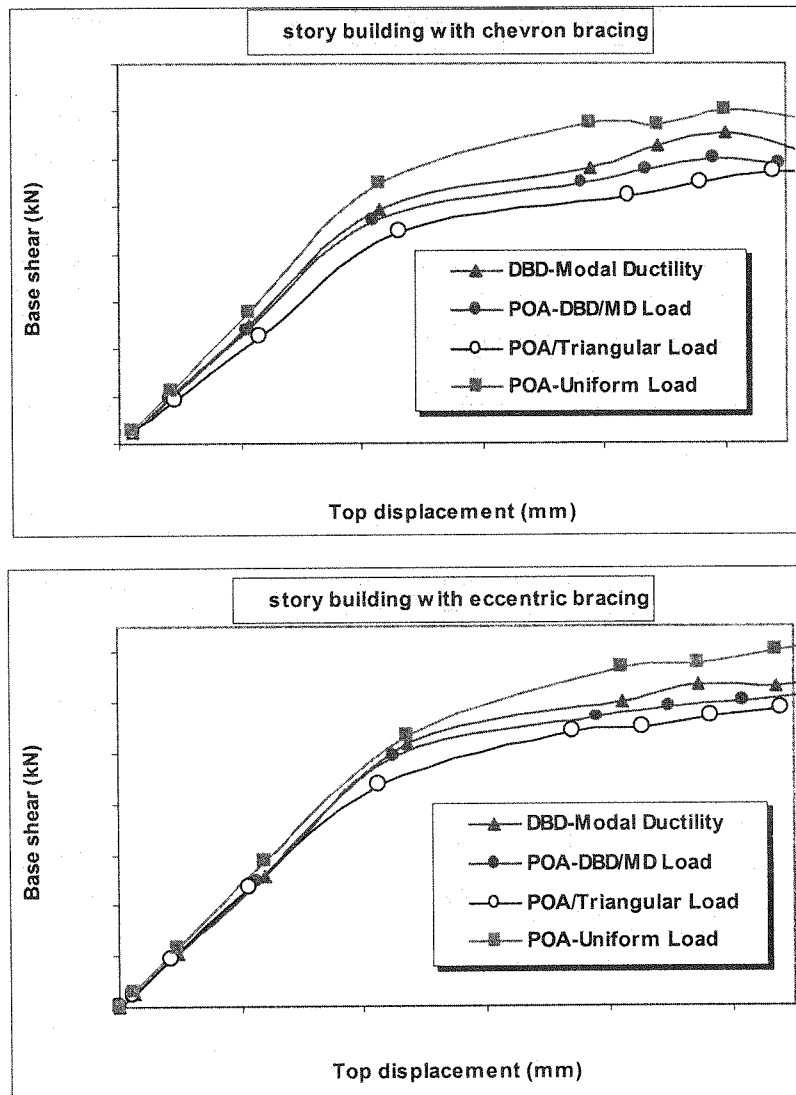


Figure (15) Base shear – top displacement curves for high rise building with different bracing systems.

- For medium and low rise buildings the code force distributions seems to be sufficient where a minimum of 80 percent of the total system mass belongs to the first mode. In high rise buildings the uniform or linear ductility demand distribution resulted in unconservative response.
- For building types studied here and similar lateral resisting systems, in which the lateral yield mechanism in the collapse limit state is known, the presented equivalent procedure for Push Over Analysis seems to be a good alternative for nonlinear static analyses and results in a great saving in the computing time and cost.
- In the braced steel buildings, where most girders are hinged at both ends, the capacity design assumptions may be more realistic. In typical structures plastic hinges may not occur in beams due to the large amount of diaphragm stiffness. So the deformation criteria such as in FEMA-357 must be checked before neglecting the diaphragm action in the displacement based procedures.
- The period of the structure used in different steps and procedures must be carefully

(a)

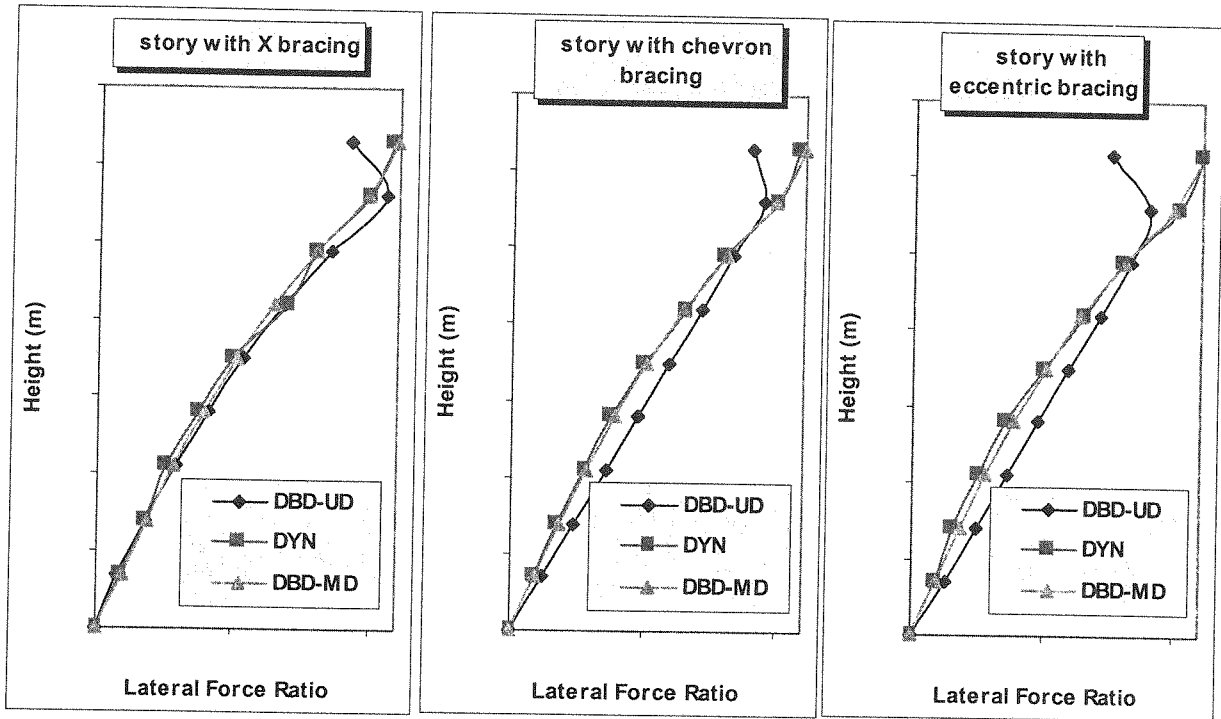
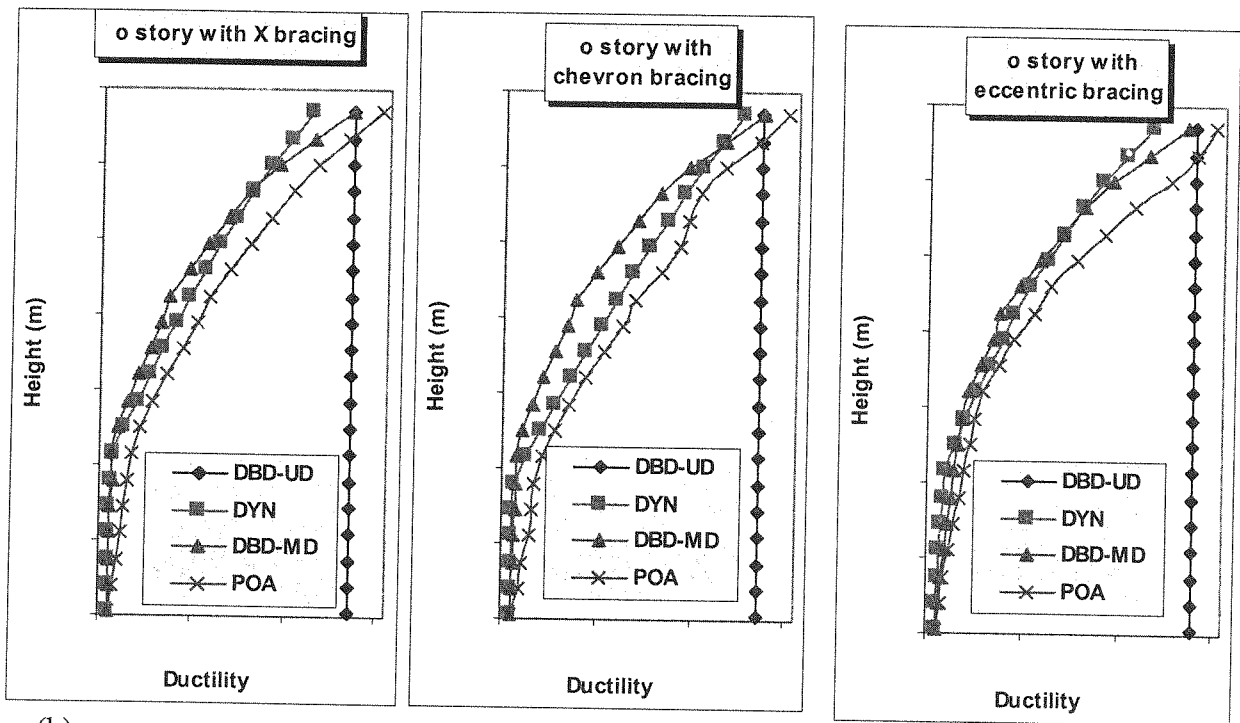


Figure (13) Lateral force ratio of mid rise buildings with different bracing systems.



(b)

Figure (14) Ductility distribution for the (a) mid and (b) high rise buildings with different bracing systems and maximum ductility capacity of 4.

strain demand in members in the structural design of the braced buildings, the participation of higher modes must be limited. This issue is generally considered in the capacity design of the structure so that the mass portion of the first mode does not decrease to values less than 70 percents or alternatively reduce the number of modes that own the 98 percents of the system mass.

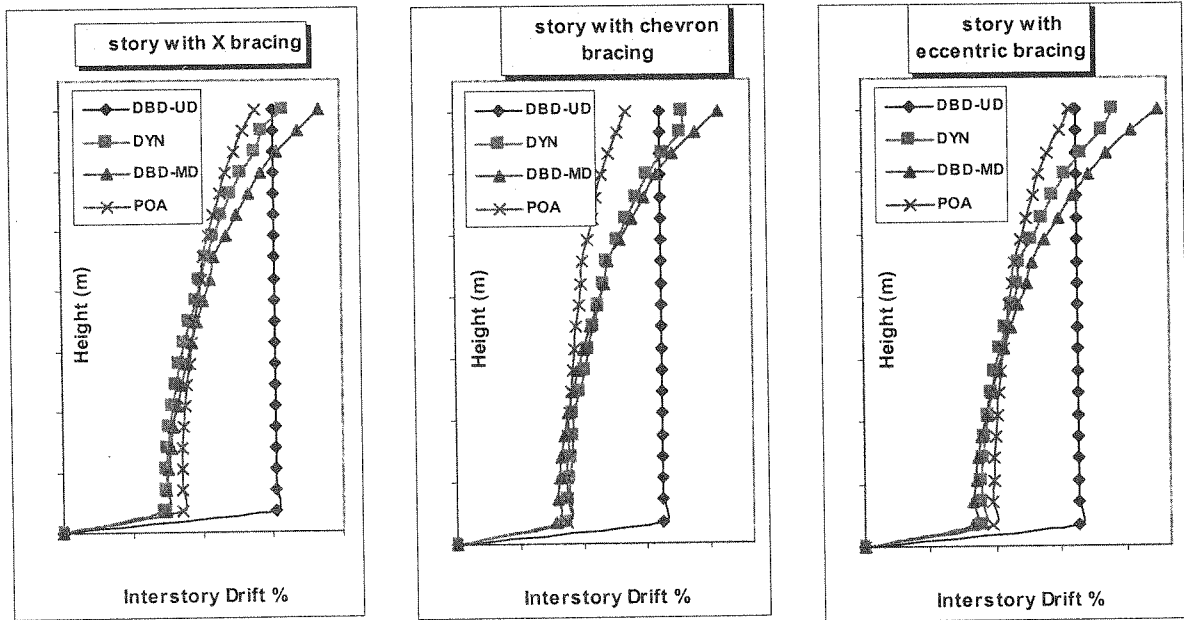
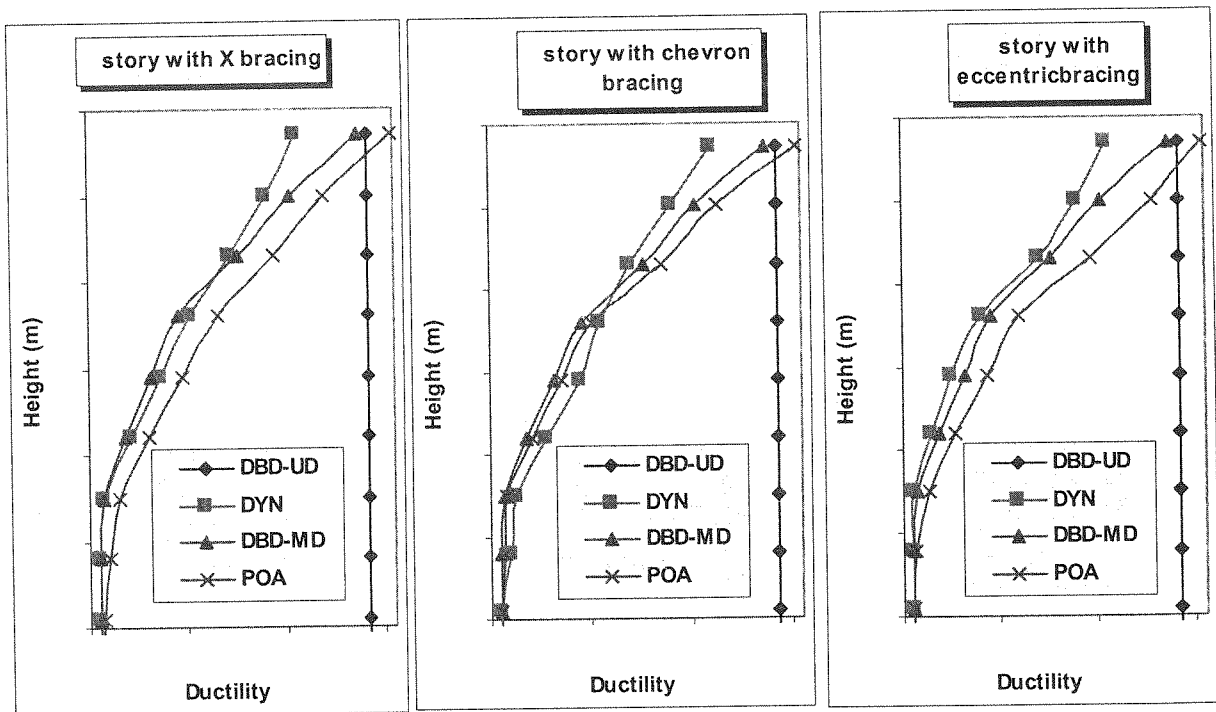


Figure (12) Interstory drift of high rise buildings with different bracing systems.



stories. This underestimation showed an average value of 35 percent for the last 5 stories while the DBD load pattern has shown a good agreement with the time history average response with a maximum of 10 percent error. Triangular force distribution can be adjusted in another way without changing the base shear so that 10 to 15 percent of the base shear is applied at the roof and the remainder distributed over the height. This procedure increases the relative strength of the upper stories and reduces the ductility demand there. Although in this way some more accurate results are obtained. Distribution of such force in the upper stories gave a more reasonable distribution of strength and ductility demand in the upper stories and approximately decreased the errors to 20 percent. Assuming the maximum ductility capacity equal to four ($\mu_{max} = 4$), the ductility distributions for all examples have been presented in figure 14. The ductility's obtained from the presented method were more adapted with the time history results comparing to the Push Over Analysis.

After a complete capacity design of each structure, the Push Over Analysis was performed using the obtained lateral load distribution, the code load distribution (Inverted triangle) and uniform load distribution. The base shear – top displacement curves obtained from these analyses has been compared to the curves obtained from the modified DBD method and shown in figures 15 for high-rise building. As shown in the figure the fixed load distribution is limited to predict higher mode effects in the post- elastic range and give unconservative results. The simple triangular or the multi-modal load pattern which is modified using equation 23 provides a conservative prediction of seismic demands in the range before first collapse and also give conservative prediction of capacity and a reasonable estimation of deformation. This load patterns slightly underestimate the demand of some buildings in the elastic range. On the other hand, it yields an acceptable estimation of shear demands at the collapse limit state. The load distribution from multimodal analysis only represents the distribution of inertia forces in the elastic range; hence higher mode effects are not entirely accounted for in the post- elastic domain. The triangular load pattern underestimates the strength in the inelastic region while the uniform pattern overestimates the strength in this region.

This study showed that for a sound designed building with known plastic mechanisms the base shear – top displacement curves obtained from the DBD method were well adjusted with the pushover curves with the same load distribution for both medium and high rise buildings: So this could be an alternative approach to obtain force – displacement relations with much less computing time and effort. For braced systems with brace yielding mechanisms this method has been successfully tested while it seems that for moment resisting systems some modifications are required.

5-Concluding Remarks

Displacement based procedures can directly lead the designer to the key design parameters such as interstory drifts and displacements. If the ductility is distributed according to the ductile design of braces over the height for example based on the elastic modal vibration of the structure, the brace characteristics will interfere with the lateral displacement. The results obtained from these studies have been summarized as follows,

- In assessing the dynamic response of braced steel buildings, brace ductility demand is more important than the target floor drift because, damage to structural and non- structural elements is directly related to the inter-storey drift. The brace type, brace hysteretic behaviour and pinching, connection details and its local eccentricities mainly control the brace ductility demand.
- The modal ductility demand distribution and the resulted force distributions give acceptable results for tall buildings compared to the dynamic analyses. However in order to avoid high

floors, the other assumptions reduce the system to a statically determinate one. All the frames in the direction of the earthquake are at their yield capacities. The additional deformations of these elements due to torsion are taken to be proportional to the distance from the center of strength (the location where the resultant of the resistance of the inelastic translator elements, here the braces, acts). So the drift criteria for structural or non- structural elements must be rechecked. Because of the elastic behaviour of the elements resisting the torsion in the perpendicular direction, it is likely that the increase in the displacement of the center of mass due to torsion is small. Therefore, a logical approach is to base the initial design on the translation of the center of mass and to modify this assumption subsequently as required. The examples presented herein were torsion ally restrained (Fig. 10), so the design ductility's have been restricted for torsion when lateral force was applied to the perpendicular direction [26]. For torsion ally restrained and redundant systems when redistribution of design actions between elements is possible, the maximum ductility limit may be increased. This allows the use of unreduced displacement ductility factor for the elements resisting torsion. In the majority of the buildings with asymmetric plan system and moderate stiffness unreduced ductility can be used for seismic design. For the presented examples the reduction in ductility capacity of the members has been neglected.

For accidental torsion it is also recommended in FEMA-356 [28] that increased forces and displacements due to this type of torsion shall be considered unless the accidental torsional moment is less than 25 percent of the actual torsional moment, or the displacement multiplier of the applied load and accidental torsion, defined as the ratio of maximum floor displacement to average floor displacement, is less than 1.1 at every floor. In our examples the maximum displacement multiplier for the applied load in the time history analysis was 1.03.

4-3-Discussions

Figure 12 shows the final results of DBD method with Uniform Ductility (UD) and Modal Ductility (MD) distributions, static Push Over Analysis with the obtained load distribution and the nonlinear dynamic analysis for interstory drifts of the nine and twenty story frames with three brace systems. As shown the modified DBD method gives conservative estimates of interstory drifts in medium and high-rise buildings through the whole height of the structure. Thus it can be used for the displacement control in the PBD while the Push Over Analysis underestimated the drifts in upper stories, which arise from its limitations in the regions where the higher mode effects govern the response. The story force ratios for mid and high rise buildings have also been presented in figure 13. The multi modal DBD has given acceptable results with respect to those obtained from dynamic analysis and estimated the force profile in a good manner. Although the ratios are not overestimated for all examples, it must be noted that the base shears were all overestimated and thus the story forces were applicable for the capacity design. Finally it is noted that, Because of the occurrence of plastic hinges in the structural model of eccentric braces, the results approximations for this type of building were more than the concentric ones compared to the dynamic response.

This study also showed that the drift pattern and force ratios in 3 story building may be well estimated by the triangular load pattern and uniform ductility distribution in the elastic range and it is slightly underestimated in the inelastic range. So there is no need for increasing ductility demand in upper stories in low-rise buildings. For the 20 story building on the contrary the code load pattern considerably underestimates the inter story drift in the upper

Table (3) Modal mass portions and effective mass ratio for different systems.

Title	1st Mode Mass %		Effective Mass Ratio %					
	Linear	Linear	X Bracing		Chevron		Eccentric	
	EVA	THA	CDC	CDN	CDC	CDN	CDC	CDN
3 story	81.1	80.5	77.3	75	76.9	73.5	76.6	72
9 story	74.3	72.2	73.3	69.4	71.5	67.8	70.8	66.8
20 story	69.7	67.9	71.9	66.2	71.1	65	69.9	64.7

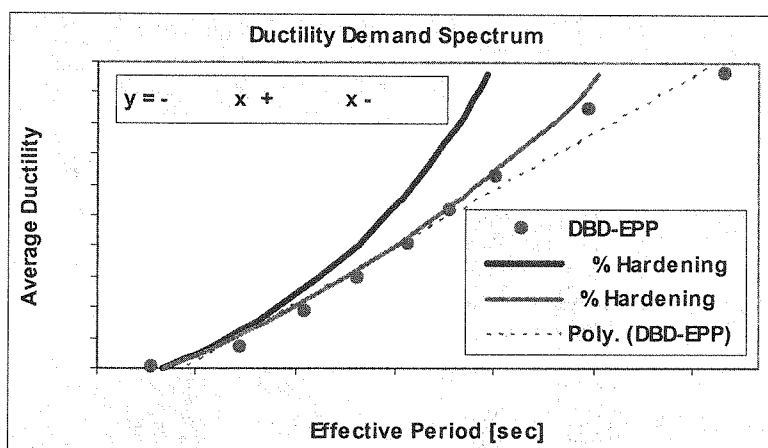


Figure (11) Effect of strain hardening on effective period in DBD method.

In order to take into account the effect of cumulative damage or the low cycle fatigue, the reduced ductility's may be used. Considering the Park-Ang model for the Damage Index (DM) the following equation can be used to calculate the reduced ductility μ due to cumulative damage corresponding to the current ultimate ductility μ_r [5],

$$\frac{\mu}{\mu_r} = \frac{DM}{1 + \tau \cdot \gamma^2 \cdot \mu} \quad (31)$$

In which parameter τ is a constant controlling strength deterioration as a function of the amount of dissipated energy which here is taken equal to 0.15. Definition for the constant parameter γ is presented in [25]. The value of DM is also taken to be equal to 1.0.

4-2-Tensional Effects

In the study of realistic behaviour of the structure a three dimensional system should be considered. The implementation of this issue leads to the consideration of torsional effects. Torsional moment and attendant shear forces in the structure are resulted from structural eccentricity defined as the distance measured perpendicular to the direction of seismic loading between the center of mass and the center of rigidity. Based on the deformation capacity of the structural system and its critical elements a design strategy for earthquake induced torsion in buildings consistent with the DBD approach has been described [26, 27] and employed here.

In the inelastic region it is assumed that the elements parallel to the lateral force have yielded due to translation and therefore the perpendicular elements must form a couple to resist the torsional moment. If no couple can form, the system is considered to be torsionally unrestrained. For torsion ally restrained systems, the elements resisting torsion are likely to behave elastically. In any case, together with the assumption of rigid body rotation of the

$$T_{eff} = T_{elastic} \sqrt{\frac{\mu}{1 - \alpha + \alpha\mu}} \quad (30)$$

This relationship did not hold true for large ductility's and over estimated the values for large period ranges. The ductility demand spectrum for presented EPP-DBD method and systems with 5 and 10 percents hardening of the initial elastic modulus have been compared in figure 11.

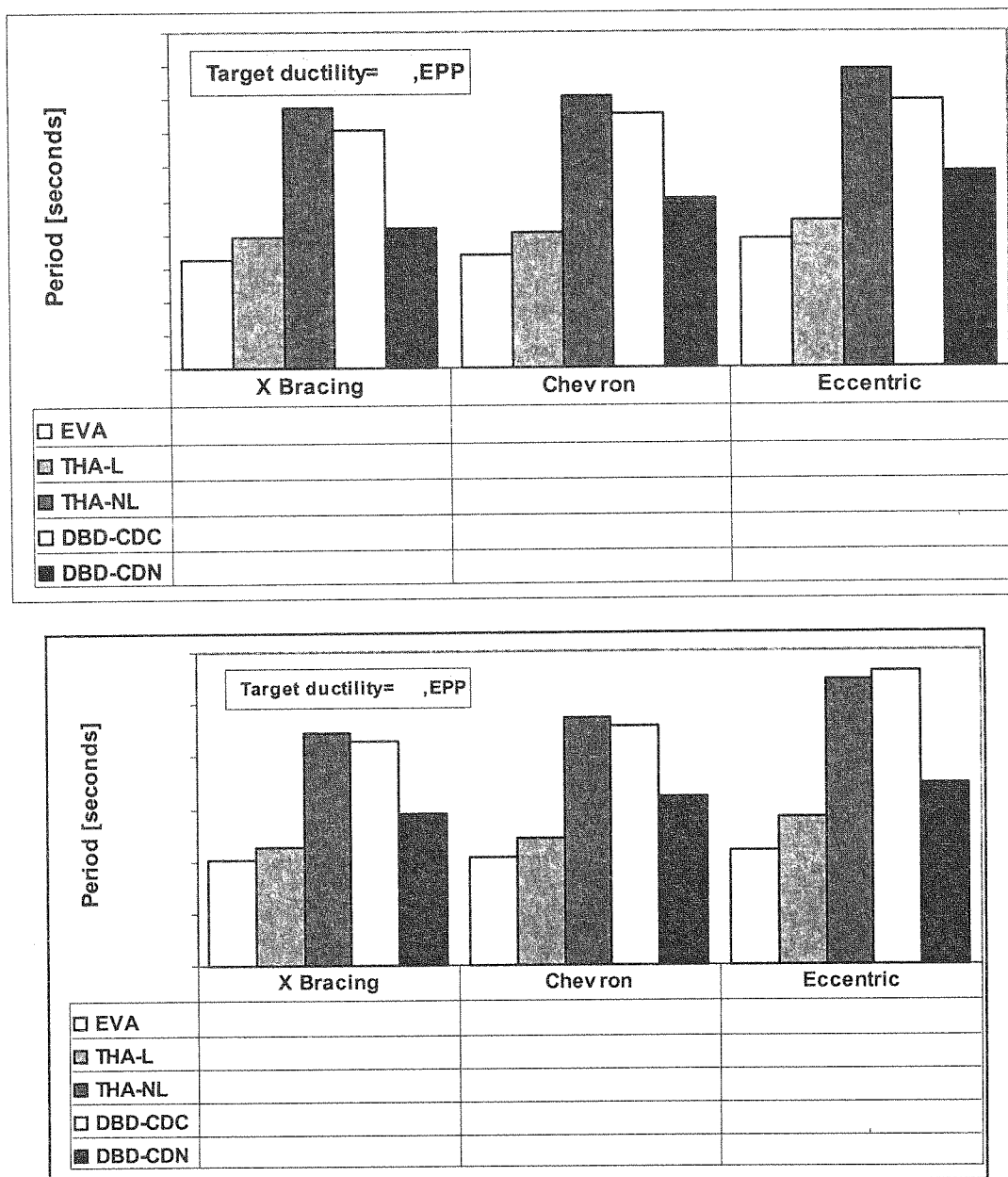


Figure (11) Effect of column deformation, vertical load and nonlinearity on natural and effective periods for (a) nine and (b) twenty story buildings [Symbols: EVA: Eigen value analysis, THA: Time history analysis, L: Linear, NL: Nonlinear, CDC: Column deformation considered, CDN: Column deformation neglected].

damage and ductility demand distribution have been discussed and the procedure to include them in the DBD method has been introduced. Column deformations have considerable effects in the seismic response of building structures and often increase the lateral displacement and ductility demand in the DBD methods. Neglecting the column deformation may also reduce the natural period obtained from eigen value analysis and may result in the reduction of ductility demand and lateral drift in the upper stories which result in unconservative design. The effect of column deformations can be counter-balanced by selecting a period less than that of T_{eff} and thus providing extra stiffness in the braces and reducing the ductility demand. Based on elastic strain energy in the structure, the lateral drift of the i -th floor, δ_{ci} , due to the elastic axial deformations of all columns below it may be obtained considering the models presented in section 3 as,

$$\delta_{ci} = \sum_{j=1}^i \frac{C_j \cdot H_j^2}{A_j \cdot E \cdot L_s} + \sum_{j=1}^{i-1} \frac{T_j \cdot H_j^2}{A_j \cdot E \cdot L_s} \quad (29)$$

Where L_s is the width of the braced frame, E is the modulus of elasticity, H_j is the story height, A_j is the area of cross-section of the column, and C_j and T_j are the compressive and tensile axial forces in the columns of the j -th story in the assumed mechanism. Based on average results of dynamic analyses, the axial stress ratio (σ/σ_y) in compression and tension, considering the effect of gravity loads, may be assumed equal to 74 and 70 percents for X braces, 76 and 73 for chevron braces and 78 and 74 for eccentric braces to have an initial estimate of the floor drift, δ_{ci} . The slight changes of these values among the height of the structure have been neglected. The effect of $P-\Delta$ may also be considered using the secondary moment induced by story weight, which increase the story lateral force. The secondary displacements have also been neglected.

In figure 11 the period of the first mode from eigen value analysis has been compared to the periods obtained from linear and nonlinear time history analyses showing the effects of vertical loads and nonlinear behaviour and also the effective periods from DBD method taking into account the effect of column deformation. The corresponding mass participations for the first mode have also been listed in table 3. The elongations in the considered periods of structures due to extensive yielding during earthquake depend on the target displacement ductility and distribution pattern and ranged between 85%, 90% and 100% for the 3 brace systems (X, chevron and eccentric bracings respectively) with respect to the elastic eigen values. The effect of vertical loads on the elastic and inelastic periods of the structure had an average value of 15% for all examples. Therefore, employment of elastic periods obtained from eigen value analysis in seismic code does not provide uniform levels of safety for different structural systems. As shown in the figure 10 the effective periods obtained from the presented DBD method for EPP systems, considering the effect of column deformations, were about 20% less than the values obtained from the nonlinear dynamic analysis. It has been also shown that the effective mass at three bracing system with or without column deformation and $P-\Delta$ effects is approximately 70 percents of the total mass. This value increases by reducing the ductility demand and yields to 80 percents for uniform ductility distribution.

The effective period T_{eff} may also be calculated in terms of average ductility μ and approximately follow the relationship; $T_{eff} = \sqrt{\mu} \cdot T_{elastic}$ for elasto-plastic systems. This simple formulation can be modified to account for the effect of strain hardening as [5],

assessment objectives in the DBD are the interstory drifts (or the distortional drift, θ_{dd} which is the ratio of drift to height), and the maximum displacement (roof displacement, Δ), that is the summation of the story drifts. In case of a uniform ductility demand distribution, Δ and θ_{dd} can be related to the effective displacement, δ_{eff} which occurs at the effective height, H_{eff} (defined in equation 20) as,

$$\Delta = \frac{H}{H_{eff}} \cdot \delta_{eff} = \Gamma \cdot \delta_{eff} \quad (27)$$

$$\theta_{dd} = \Gamma_{dd} \cdot \frac{\Delta_{eff}}{H} \quad (28)$$

Where H is the total height of the building. For the model discussed in this paper the coefficient Γ is different from H/H_{eff} due to the nonlinear ductility distribution over the height of the structure. The average of this parameter for given examples are presented in table 2 for target ductility value of 3. The corresponding values of effective height that were used to consider the effect of higher modes in the upper stories are also presented in the table. As shown, the coefficient Γ increases by decreasing the building height. The value also decreases by changing the brace system from concentric to eccentric. For low and medium rise buildings equation 26 is approximately satisfied. On the contrary in case of tall building this equation underestimate the value of Γ and could not be used for performance design.

Table (2) Values of Γ and effective height.

$\mu_{TARGET}=3$	Low Rise Building		Mid Rise Building		High Rise Building	
	Γ	H_{eff}/H	Γ	H_{eff}/H	Γ	H_{eff}/H
X Bracing	1.90	0.52	1.71	0.58	1.31	0.68
Chevron	1.87	0.53	1.67	0.60	1.30	0.70
Eccentric	1.82	0.55	1.62	0.61	1.27	0.72

The second seismic displacement coefficient, Γ_{dd} is typically in the order of 1.5~3 for regular buildings and can be equal to the number of stories in the building in the extreme situation of a soft-storey mechanism [24]. Finally the displacement demand should be checked with the code requirements ($\Delta = \Delta_y + \Delta_p \leq \Delta_{code}$ or $\theta_{dd} = \theta_y + \theta_p \leq \theta_{code}$). This parameter lied in the range of 0.7 to 0.75 of the building height for different examples and increased slightly by increasing the target ductility. This parameter was not also too sensitive with respect to the height of the structure.

4-1-Effective Period Tracing

In the DBD changes in the lateral displacement profile result in period shifting and consequently changes in the design forces. In this section the factors affecting on period including column deformations, gravity loads and $P-\Delta$, strain hardening, cumulative

Figure 11 shows the effect of the ductility demand distribution on story force and story drift using modal ductility distribution and equations 21 and 22 for a nine-story building with eccentric bracing. The maximum ductility is assumed to be 2 according to fig. 8. It has been shown that the lateral story force has not been so sensitive to the ductility pattern but the displacement and drift directly change with the ductility in the DBD and equation 21 with $a=-3$ and equation 22 with $b=3$ may be acceptable comparing to the dynamic analysis results. In table 2 the effect of ductility pattern on DBD parameters (Effective parameters on the equivalent SDOF structure) has also been presented. As shown the effective damping, total base shear, mass and effective height ratio which may be assumed as the representative for lateral force distribution are not sensitive to the ductility distribution over height and just depend on the maximum ductility value.

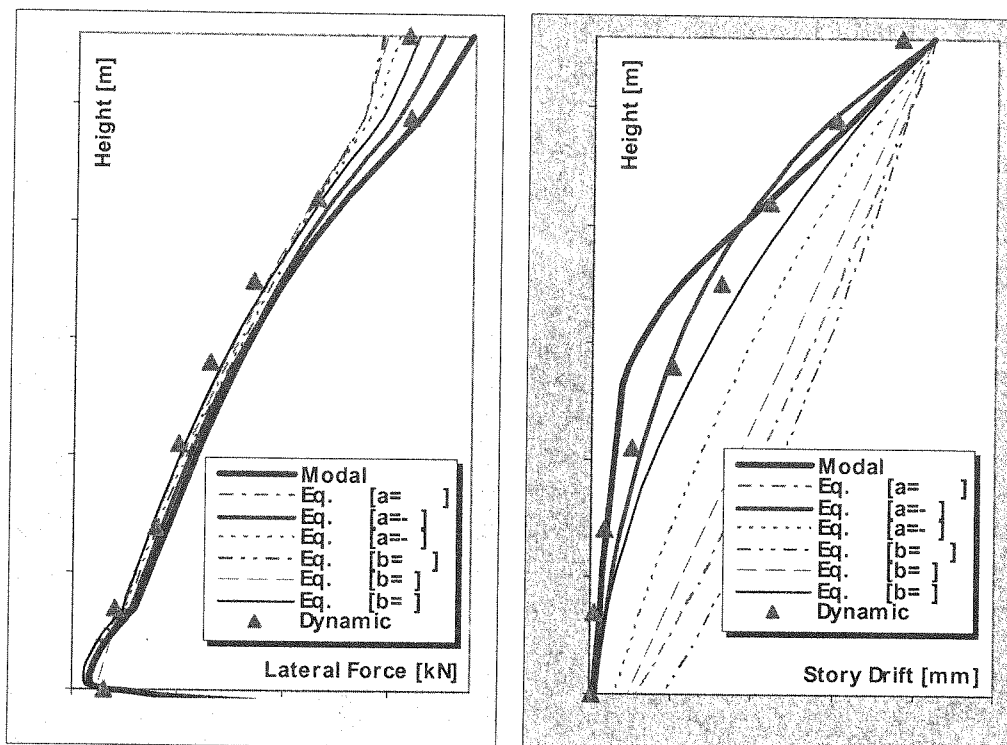


Figure (11) Effect of ductility demand distribution on story force and drift.

Table (2) Effect of ductility demand distribution on DBD parameters.

Effective Parameters	Units	Modal Pattern	Exponential (Equation 21)			Polynomial (Equation 22)		
			a=0.01	a=-3	a=-1	b=0.7	b=2	b=3
Effective Period	Sec	0.85	1.30	0.92	1.14	1.35	1.25	1.01
Effective Damping	%	4.36	4.79	4.42	4.65	4.81	4.74	4.53
Mass Ratio		0.71	0.73	0.71	0.72	0.74	0.72	0.70
Effective Stiffness	N/mm	13601	5986	11783	7622	5658	6427	9550
Effective Displacement	Mm	92	134	97	116	140	128	104
Effective Height Ratio		0.73	0.73	0.73	0.73	0.72	0.73	0.74
Total Base Shear	KN	798	674	756	683	685	674	705

The relationship between member strains or member plastic rotations with the inter-story drifts has been determined (equations 13 to 19); therefore both local and global performance criteria may be checked for such a design method. The most commonly used performance

with five percent strain hardening or second modulus $E_s = \alpha.E, \alpha = 0.05$. The dead load is assumed to be 3.9 kPa. And the reduced live load 1.4 kPa at floor levels. At roof level these values are assumed to be 3.2 kPa. And 1.0 kPa. Respectively. The assumed data may be sufficient for DBD, but for the nonlinear push over and time history analyses the detail design of the members must also be available. This has been performed using the capacity design procedures and was performed using SAP2000 [21] commercial program. To provide strong column-weak beam connection in the capacity design of member connections, the following relationship was satisfied according to LRFD-1996,

$$\frac{\sum Z_{col} (\sigma_{y,col} - P_{u,col} / A_{col})}{\sum (Z_{beam} \cdot \sigma_{y,beam})} \geq 1.0 \quad (26)$$

Where A is cross sectional area of the column, σ_y is specified minimum yield strength for beam and column, P_u is required axial strength in column in compression, and Z is plastic section modulus of the beam. This equation need not be satisfied when $P_{u,col} < 0.30 \sigma_{y,col} \cdot A_{col}$. The contribution of diaphragm action and nonstructural components such as infill in stiffness and strength of the system have been neglected noting that for eccentric bracings the diaphragm should not be too rigid in order to allow the formation of plastic hinges in the link beam. $P-\Delta$ Effect has also been considered in DBD, Push Over Analysis and dynamic analyses. The modified strength reduction factors for MDOF structures taking into account the reductions due to structural over strength have been calculated based on the equations proposed in [23]. The effects of cumulative damage may also be considered using the idea presented in [5] that has been discussed subsequently. Nonlinear dynamic analyses have been performed using DRAIN2DX [22] program using three-selected earthquake record, which were compatible with the obtained response spectrum shown in fig. 2.

Table (1) Geometric data for numerical examples (Dimensions in meter).

n story	H_1	$(n-1) \cdot H_1$	L_{s1}	$No \cdot L_{span1}$	L_{s2}	$No \cdot L_{span2}$	l_l
3 story	3.5	2*3.5	2(4.0)	2*4	2(3.5)	2*4	1.5
9 story	4	8*3.5	2(4.2)	2*4.2	2(3.5)	2*4	1.5
20 story	4	19*3.5	2(4.2)	3*4.2	2(3.5)	3*4	1.5

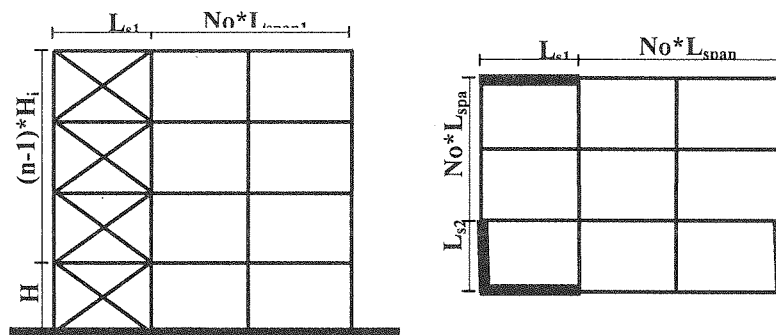


Figure (10) Geometric data for all numerical examples.

$$\Phi(h) = \frac{h}{H} \quad (24)$$

And therefore the assumption of uniform ductility demand distribution among height gives reasonable results. For high rise buildings for which $3 < \frac{H}{L}$ the shape function will lead to a flexural pattern shown in fig. 9-c with the following equation [20],

$$\Phi(h) = 1 - \text{Cos}\left(\frac{\pi \cdot h}{2H}\right) \quad (25)$$

For this building type, the demands are overestimated in lower stories due to the flexural displaced shape and underestimated in upper stories due to the higher modes effects. For these types of structures and those with possible special mechanisms such as soft story mechanism the presented model may be more reliable.

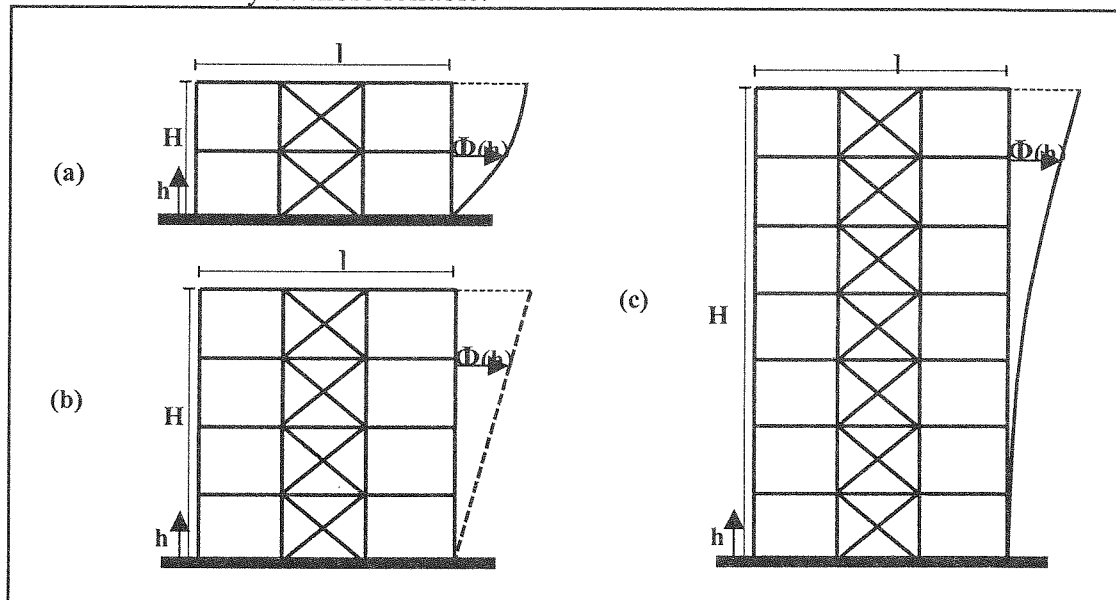


Figure (9) Lateral displaced shape for different buildings.

The final displaced shape is obtained by multiplying the initial profile obtained from the mechanism models, introduced in the previous section, by ductility demand distribution. The maximum ductility capacity of the each story (defined as the ratio of maximum displacement capacity and yield displacement of the story) must also be determined. This parameter defines the limit state or the performance point. For concentric and chevron braced frames this is governed by the capacity of the brace to beam connection and for eccentric braces the plastic rotation capacity of the link beam defines the ductility. Some modifications for the effects of strain hardening and cumulative damage can also be assessed in the DBD method that has been discussed in the next section.

4- Numerical Examples

In this section, the presented modifications have been verified through some numerical examples including three, nine and twenty story-braced frames. The geometric data of the models are presented in table 1 and fig. 10. The steel properties are, yield stress $\sigma_y = 245\text{MPa}$, initial elastic modulus $E = 2.10e5\text{MPa}$ with a bilinear nonlinear behaviour

$$\phi_{\mu\{EXP\}} = \mu_{\max} \cdot \frac{1 - EXP(-a h/H)}{1 - EXP(-a)} \quad (21)$$

The third function is a simple polynomial function with parameter b as,

$$\phi_{\mu\{P\}} = \mu_{\max} \left(\frac{h}{H} \right)^b \quad (22)$$

The comparison of various ductility patterns using the mentioned functions has been plotted in fig. 8. The Initial or elastic shape of the buildings may be assumed using the following conventional relation ships. If H is the total building height and L is the total building width, for low rise buildings where $H/L < 3/2$ the governing spatial shape function would be,

$$\Phi(h) = \text{Sin} \left(\frac{\pi \cdot h}{2H} \right) \quad (23)$$

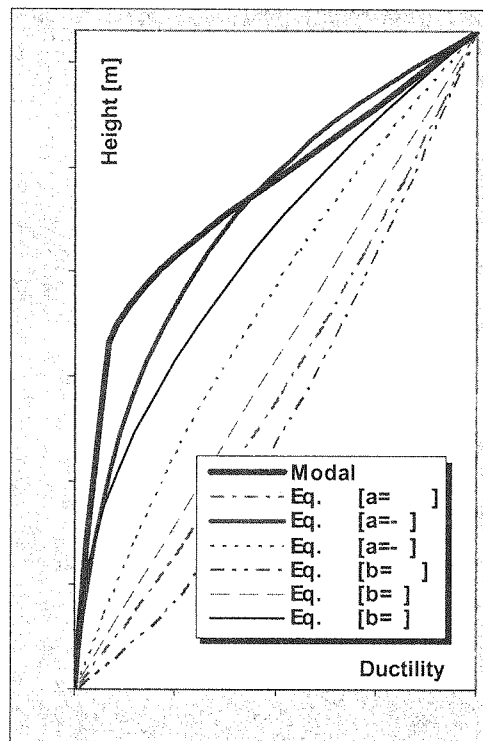


Figure (8) Various ductility distribution patterns considered in the study.

which results in a shear deflection pattern as shown in fig. 9-a. For these types of structures, the assumption of uniform ductility distribution underestimates the displacement and inter-story drift demands. For medium rise buildings in which $3/2 < H/L < 3$ the lateral deflection have an approximately linear distribution, shown in fig. 9-b, as,

2-2-Ductility Demand Distribution

In the conventional DBD in which the ductility is assumed uniform over the height, the effective stiffness would not change with the ductility. If the ductility is distributed according to the ductile design of braces over the height for example based on the elastic modal vibration of the structure, the brace characteristics will interfere with the lateral displacement. The increase in the resulted ductility in comparison with the uniform distribution, will cause reduction in the effective mass and results in an increase in the effective period due to the rise in effective displacement and thus reduce the resulted effective stiffness of the substitute SDOF structure. In the presented DBD method, the lateral displaced shape of the structure is modified using multi-modal, polynomial and exponential distributions of ductility over the height of the structure in order to take into account higher mode effects and combined shear and flexural lateral deformations. Higher mode effect cause considerable changes in the dynamic response of large period or flexible structures such as tall buildings. Besides, the ductile behaviour of the building also results in considerable increases in the system period. This issue has been discussed in the parametric study. In low-rise buildings the shear behaviour often governs the response and in medium rise buildings a combined shear and flexural deformation is normally expected.

For modal distribution of ductility it is assumed that the distribution is approximately conformed to the some first mode shapes which have a more than 98 percents of the system mass. For most of the structures, the first three modes of a cantilever shown in fig. 7 with known equations may be assumed or alternatively an elastic modal analysis of the structure can be performed and then a mode combination procedure followed. However in order to avoid high strain demand in members in the structural design of the braced or wall buildings, the participation of higher modes must be limited. This issue is generally considered in the capacity design of the structure so that the mass portion of the first mode does not decrease to values less than 70 percent or alternatively reduce the number of modes that own the 98 percent of the system mass. In the presented study, as an alternative approach and in order to conform to the capacity design criteria, the effect of higher modes on the ductility demand distribution in the lower stories has been neglected as shown in fig. 7, the stories below the effective height where the lateral force acts and can be calculated using equation 6 as,

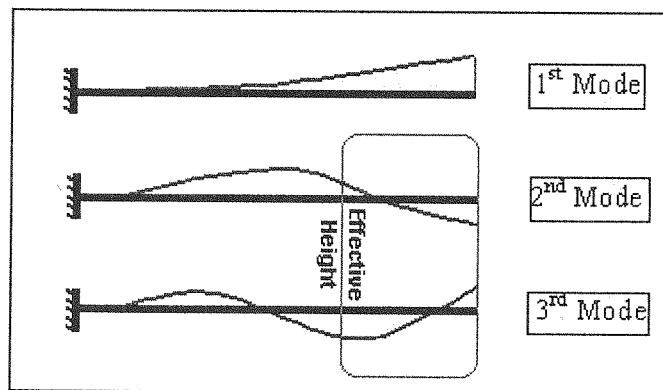


Figure (7) The first three mode shapes of cantilever beam used in the analyses

$$H_f = \frac{\sum_{i=1}^n f_i \cdot H_i}{V_b} \quad (20)$$

The second selected pattern is an exponential function with parameter a as follows,

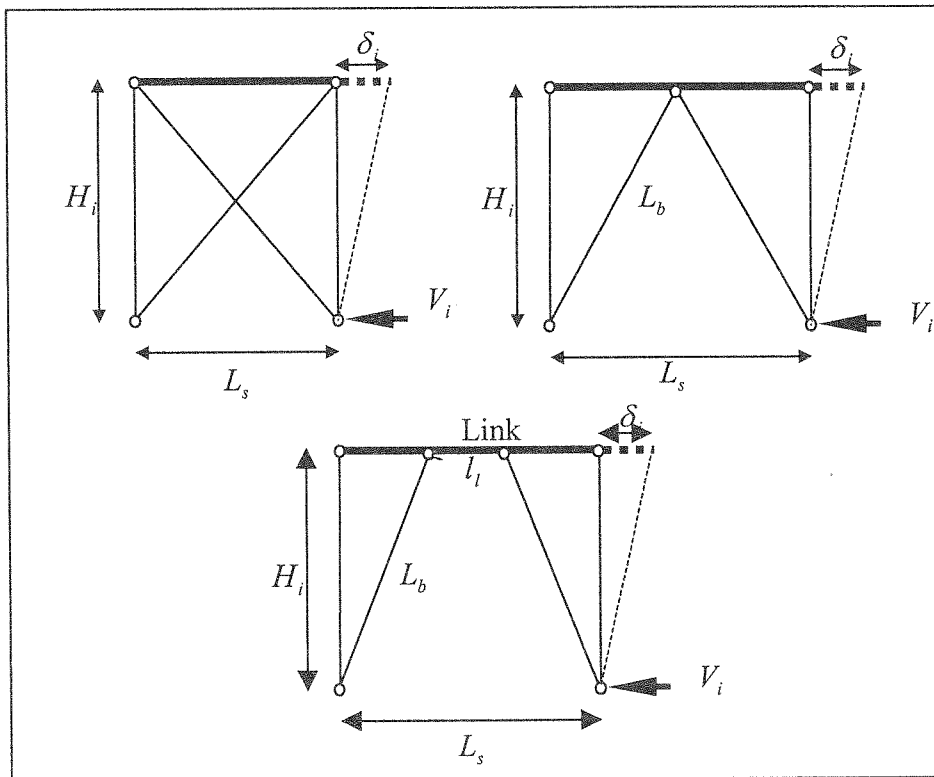


Figure (5) Structural models for X bracing, chevron bracing and eccentric bracing systems.

For small length link beams, the shear mechanisms are formed while in moderate length link beams moment plastic hinges are generally formed. The latter case has been considered here. The value of θ_p is generally related to the connection and link beam details.

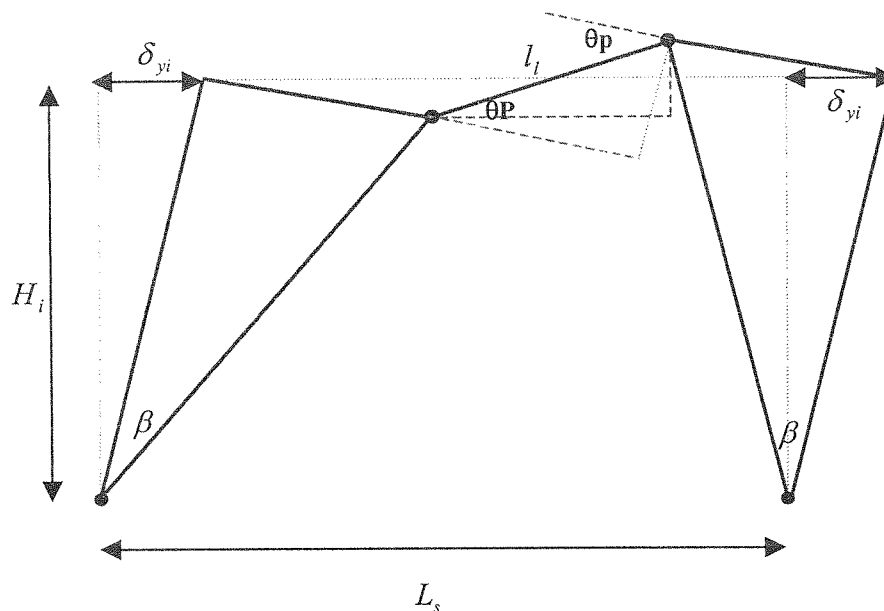


Figure (6) Yielding mechanism model for eccentric bracing system.

For concentric X bracing systems as shown in fig. 5-a the lateral story displacement δ_i can be written as a function of story shear V_i , brace span L_s , brace length L_b , brace sectional area A_b and elastic section modulus E as,

$$\delta_i = \frac{V_i \cdot L_b^3}{E \cdot A_b \cdot L_s^2} \quad (12)$$

Using equation 12 and considering the relation $\frac{L_s}{L_b} = \frac{V_{yi}}{\sigma_y \cdot A_b}$ from figure 5, the story yield displacement δ_{yi} in a concentric braced frame can be obtained as,

$$\delta_{yi} = \frac{V_{yi} \cdot L_b^3 \cdot \epsilon_y}{\sigma_y \cdot A_b \cdot L_s^2} = \frac{L_b^2 \cdot \epsilon_y}{L_s} \quad (13)$$

Which does not depend on the brace sectional area. Similarly, for the Chevron bracing shown in fig. 5-b, the same equations may be obtained as follows,

$$\delta_i = \frac{2V_i \cdot L_b^3}{E \cdot A_b \cdot L_s^2} \quad (14)$$

$$\delta_{yi} = \frac{2V_{yi} \cdot L_b^3 \cdot \epsilon_y}{f_y \cdot A_b \cdot L_s^2} = \frac{2L_b^2 \cdot \epsilon_y}{L_s} \quad (15)$$

It is apparent that for Chevron bracing the displacement shape in yielding case of the structure is independent of the brace sectional properties. Thus for the concentric systems, an equal span and story height result in a linear deformed shape of the structure over the height at yield condition.

For eccentric bracing systems (fig. 5-c), the lateral displacement depends on plastic rotation capacity of the link beam, θ_p , and can be expressed through the following equations with reference to fig. 6,

$$\delta_{yi} = H_i \cdot \sin(\theta) - l_i \cdot (1 - \cos(\theta_p - \theta)) \quad (17)$$

$$\theta = \pi - \beta - \text{ACos} \left[\frac{L_s^2 - l_i^2 + 2l_i \cdot L_s \cdot \sin(\beta - \theta_p)}{2L_s \cdot L_b} \right] \quad (18)$$

Where θ_p is defined as a function of section plastic moment M_p and plastic stiffness K_p as,

$$\theta_p = \frac{M_p}{K_p} = \frac{V_i \cdot H_i}{2K_p} \quad (19)$$

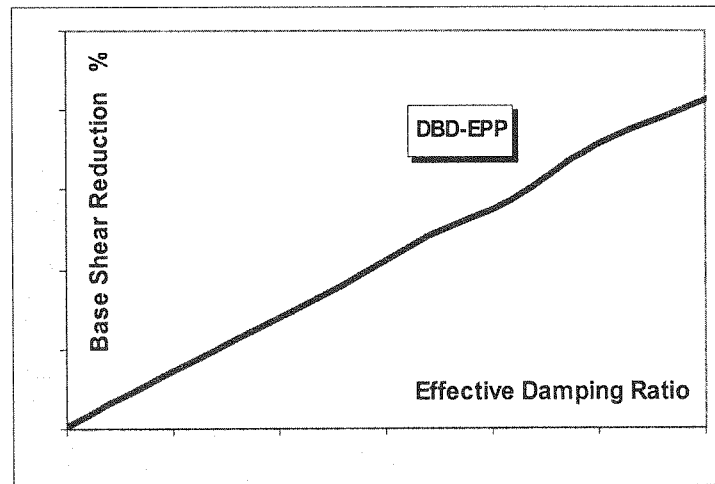


Figure (4) Reduction of design base shear due to the consideration of damping in the design spectrum.

2-Structural Mechanism Models

In regular buildings usually the first mode of elastic vibration is presumed to approximate the inelastic displacement profile. However, in areas with high seismicity it is needed to include more nonlinear behavior possibly by changing the design limit states to life safe or near collapse limit states. The seismic standards also recommend to special lateral resisting systems with ductile behaviour for structures in these zones. On the other hand, some issues may significantly shift the first mode profile for example higher mode effects in high-rise buildings and unpredicted plastic hinge formations. Therefore, it is necessary to conduct more comprehensive methods to take these effects into account. In recent years many researchers have tried to find engineering procedures to do this task but each had some limitations. Studies have shown that Push Over Analysis is limited to low to medium rise buildings and is not recommended for high rise or flexible structures in which higher mode effects are not negligible and may govern the dynamic response [19]. Other existing methods such as the Capacity Spectrum Method and the N2 Method have similar limitations. In the first part of this section, simple plastic models for the story or local ductility of braced steel building with concentric and eccentric bracing systems have been proposed. In the second part, various functions for ductility demand distribution over the height of the structure have been introduced and then they have been verified by comparing to dynamic analysis results through various numerical examples.

2-1-Lateral Story Yield Mechanism

In the presented DBD method, the story mechanisms are presumed to occur due to the yielding of the lateral resisting system. Therefore, the failure mechanism of the stories that depends on the structural geometry, yield strains and lateral load resisting system may be determined. In the case of a capacity-designed structure, the lateral mechanism can be predicted with good approximation. For steel braced frames considered in this study, the mechanisms are assumed to form by yielding of braces in concentric systems and by flexural yielding of link beams in eccentric systems as shown in figure 5. In these models one column lift is assumed for each story, which means that no rotational column plastic hinge is produced.

2-1-Effective Damping for DBD

Assuming a single displacement cycle based on the ultimate displacement the following well-known relationship between ξ_{eff} and the ductility demand μ for Elastic-Perfectly Plastic (EPP) behavior is obtained (Equivalent Energy Method [16]),

$$\xi_{eff} = \frac{2}{\pi} \left(1 - \frac{1}{\mu} \right) + \xi_{elastic} \quad (10)$$

Where $\xi_{elastic}$ stands for the damping of the elastic structure. The equivalent viscous damping for bilinear systems with strain hardening ratio α and ductility μ may also be determined using the following equation [5],

$$\xi_{eff} = \frac{2}{\pi} \left(\frac{(1-\alpha) \cdot (\mu-1)}{\mu - \alpha\mu + \alpha\mu^2} \right) + \xi_{elastic} \quad (11)$$

Assuming 3.0 percent elastic damping ratio for steel structures, the effect of hardening on the effective damping values has been presented in figure 3.

The effective damping obtained above which is greater than the elastic viscous damping due to the hysteretic behaviour is then used to get the effective period from the displacement spectrum. The presented spectrum shown in fig. 2 may be modified for other damping values using the EC8 [18] factor $\sqrt{\frac{7}{2+\xi}}$. Greater value of damping results in a greater effective period in the displacement spectrum and thus less base shear for the design. However it has been shown that for regular buildings, neglecting of higher damping values in the design spectrum will almost result in a conservative design. The average design base shear reductions for our numerical examples, discussed in section 5, have been presented in figure 4. As shows in the figure, this conservation may result in uneconomic design.

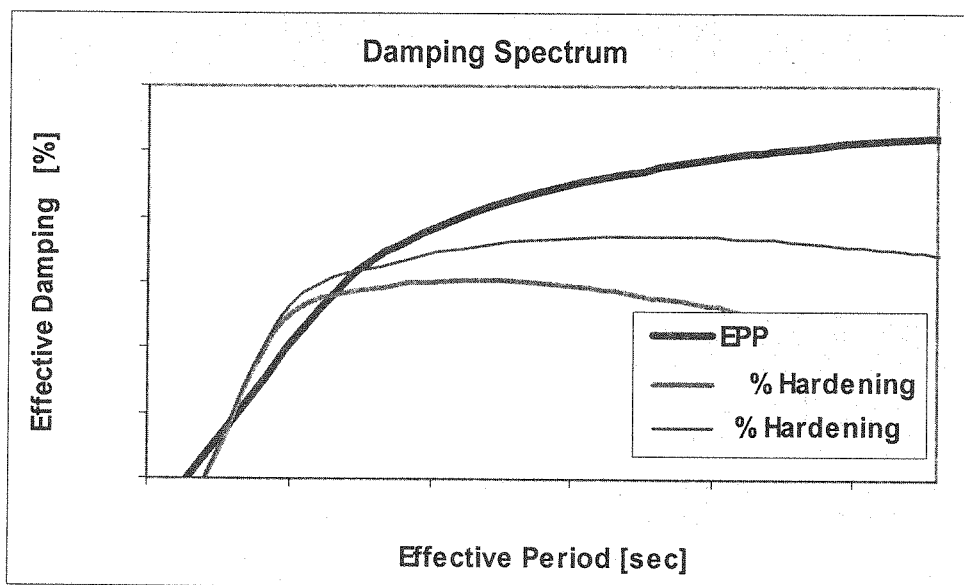


Figure (3) Damping spectrum for EPP, 5 and 10 percent hardened systems.

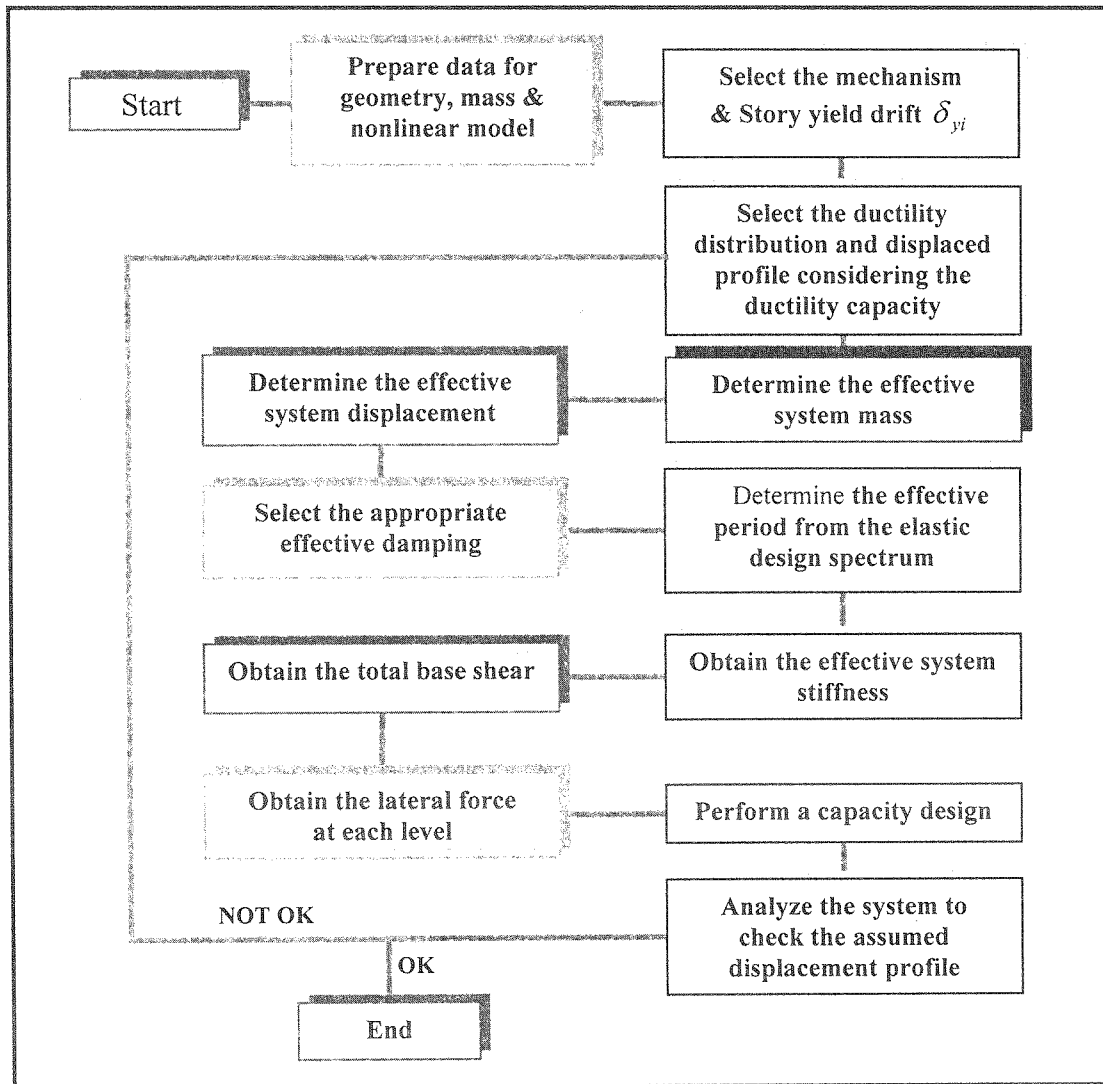


Figure (1) summarized procedure for direct displacement based design method.

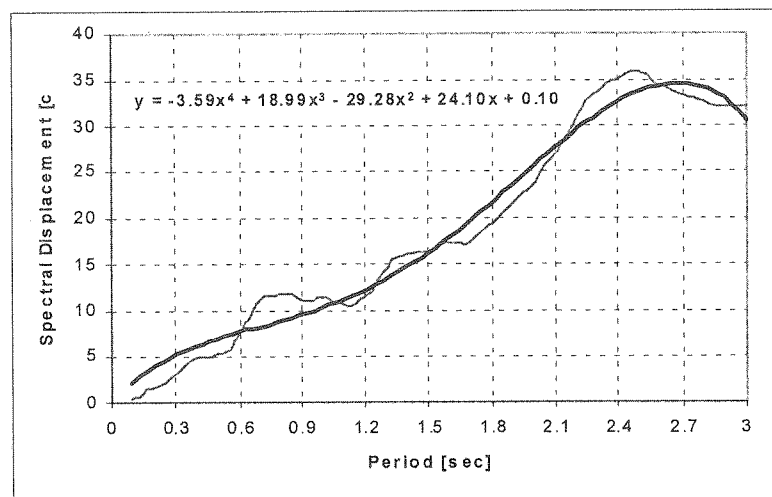


Figure (2) The displacement spectrum based on filtered Iran earthquakes and the design curve.

Where μ_i is the story ductility demand and δ_{yi} is the story yield displacement. The problem is now how to determine these two parameters. The story yield displacement δ_{yi} may be obtained by defining the story yield mechanism and has been discussed later in section 3. Determination of the ductility distribution through the height of the structure has also been discussed in section 3. Finally for detail design of the structure the base shear is obtained as $V_b = K_{eff} \cdot \delta_{eff}$ and then the story forces f_i are computed using equation 6. Then the capacity design of the structure can be started considering the ductility capacities. This capacity-designed structure may then be verified using the time history or static push over analyses. The design procedure has been summarized in Fig. 1.

1-1-Design Displacement Spectrum

In force based design (FBD) earthquake induced forces are determined from the acceleration response spectrum, which is obtained from earthquake accelerogram. Earthquake accelerograms are best suited for short period ranges (0.1 to 0.5 seconds), in which the acceleration response spectrum is sensitive to the excitation. In the current code design procedures, for a given elastic design spectrum the maximum strength reduction factor should be computed so as to avoid larger ductility demands. In, have good precision. Velocity response spectrum extends the period range to about 2.5 seconds. This type of spectrum has more close relation with structural damages [16]. In the DBD method, the displacement response spectra are used. For ductile structures, the period of the substituted structure may increase to more values (for example to 4 seconds). Thus the displacement response spectra, which have acceptable precision in the long period ranges, may be more appropriate for this type of buildings. Design displacement spectra may be generated by integrating numerically the response of a SDOF system subjected to appropriate ground motions. Linear displacement response spectrum is obtained by applying the factor $1/\omega^2$ to the acceleration response spectrum. Although the elastic acceleration design spectrum is available from codes, it is not appropriate to be a basis for the determination of the elastic displacement design spectrum because the resulted displacement increases with the period even at longer periods. For large period ranges (e.g. more than 3 seconds) slight changes in acceleration response spectrum often results in a horizontal line in the displacement response spectra and so the period values may be undefined for equal displacement values. For these ranges it is recommended (e.g. EC8) to substitute this line with a decreasing slope line to a specific value of earth displacement but more studies is still needed for this problem.

In this paper, a displacement response spectrum has been obtained through a deterministic procedure based on acceleration data for Iran earthquakes. These accelerograms were selected from more than 2000 records for different stations and earthquakes in Iran. The near field records were omitted and the accelerograms with medium to high magnitude (minimum 5 degrees in Richter scale) were selected. Using an Artificial Neural Network simulator (a committee neural simulator including competitive and back error propagating networks), prepared by the authors [17], the records were categorized according to their shapes (duration, sequence of peaks and their amplitude) by the competitive network to four categories. Each category represented a soil type thus the design displacement spectra for each soil type was obtained. The spectrum with 5 percent damping for soil type C (or II according to Iranian seismic code) has been presented in Fig. 2. A four-degree polynomial function has been matched to the data with a 0.98 standard deviation as shown in the figure. This equation was used to calculate the effective displacement in the numerical examples.

In which n stands for number of stories, a_{eff} is called the effective acceleration of the equivalent SDOF system and δ_i , a_i are the story displacement and acceleration respectively. Using equation 4, the base shear can now be determined in terms of the multi story structure and the equivalent system parameters as,

$$V_b = \sum_{i=1}^n f_i = \sum_{i=1}^n m_i \cdot a_i = \left\{ \sum_{i=1}^n m_i \cdot c_i \right\} \cdot a_{eff} = m_{eff} \cdot a_{eff} \quad (5)$$

Which leads to the definition for the effective mass as $m_{eff} = \sum_{i=1}^n m_i \cdot c_i$. The lateral force at each level, f_i may also be determined using equations 4 and 5 as,

$$f_i = \frac{m_i \cdot \delta_i}{\sum_{j=1}^n m_j \cdot \delta_j} V_b \quad (6)$$

Equating the external works for the two systems, $V_b \cdot \delta_{eff} = \sum_{i=1}^n f_i \cdot \delta_i$ and using equation 6, we can obtain the definition for effective displacement as,

$$\delta_{eff} = \frac{\sum_{i=1}^n m_i \cdot \delta_i^2}{\sum_{i=1}^n m_i \cdot \delta_i} \quad (7)$$

The effective stiffness of the substitute SDOF system may also be obtained by entering the effective displacement into the displacement response spectrum with appropriate damping value and then substituting the obtained effective period and effective mass from equation 5 into the following equation,

$$K_{eff} = \frac{4\pi^2 m_{eff}}{T_{eff}^2} \quad (8)$$

The effect of story ductility may be considered substituting δ_i defined in equation 4 with the following relationship,

$$\delta_i = \mu_i \cdot \delta_{yi} \quad (9)$$

associated with effective viscous damping and the latter is directly constructed based on relations between reduction factors and ductility.

In this paper the idea of direct DBD method has been briefly reviewed for multi story steel building structures. In this method the design force distribution among the height of the structure is obtained based on various ductility demand distributions derived from modal characteristics of the structure and mathematical formulations. The method has been applied to the steel braced frames with concentric and eccentric bracing systems in low, medium and high-rise buildings. The plastic mechanism for each system has also been modeled and the efficiencies and deficiencies of each have been discussed through various numerical examples. The effect of yields mechanisms and ductility demand patterns for various building types on the equivalent SDOF parameters have been investigated compared to the time history analysis results to find the sensitive parameters. A design displacement spectrum has also been made for the parametric study based on the Iran earthquakes. The procedure also contains the various factors affecting the dynamic response. It has been shown that this method is capable of predicting the response of braced frames especially high-rise buildings in an efficient and robust manner.

1-DBD Approach for Multi Story Steel Frames

The formulation of the direct DBD has been presented for multi story steel frames including the effect of ductility demand on the lateral displacement profile. Conventional DBD of multi story buildings is based on the generation of equivalent SDOF system or substitute structure concept. For this purpose, it is assumed that the structure vibrates in a pre-defined harmonic displaced shape. The base shears and the works developed by lateral external forces are also assumed the same for both equivalent and main structures [7-15]. Consider the relative displacement vector $\{\delta(h,t)\}$ for the multistory building with total height of H expressed in a decomposed form of displacement and time and assume a harmonic response with amplitude Δ for the system. We can write,

$$\{\delta(h,t)\} = \Delta \cdot \text{Sin}(\omega t) \cdot \{\Phi(h)\}, \quad 0 \leq h \leq H \quad (1)$$

Which results in an acceleration vector $\{a(h,t)\}$ proportional to the assumed normalized displacement vector $\Phi(h)$ as follows,

$$\{a(h,t)\} = -\Delta \cdot \omega^2 \cdot \text{Sin}(\omega t) \cdot \{\Phi(h)\} = -\omega^2 \cdot \{\delta(h,t)\} \quad (2)$$

In order to obtain the equivalent system parameters, we define the normalized displacement vector $\{c(h,t)\}$ as,

$$\{c(h,t)\} = \frac{1}{\delta_{eff}} \{\delta(h,t)\} \quad (3)$$

Where δ_{eff} is called the effective displacement. From equation 2 and 3 we may have,

$$c_i(h,t) = \frac{\delta_i(h,t)}{\delta_{eff}} = \frac{a_i(h,t)}{a_{eff}}, \quad i = 1, 2, \dots, n \quad (4)$$

DBD Approach for Investigation of Ductility Demand Distribution Effect in Braced Steel Frames

M.Tehranizadeh

Professor

Department of Civil and
Environmental Engineering,
Amirkabir University of Technology

M.Safi

Ph.D. Student

Department of Civil Engineering,
Amirkabir University & Faculty Member of
Power & Water Institute of Technology

Abstract

A modified Displacement Based Design (DBD) procedure has been proposed to account for ductility demand distribution through the height of the building. In this method the design force distribution among the height of the structure is obtained based on various ductility distributions derived from modal characteristics of the structure and mathematical formulations. The method has been applied to the steel braced frames with concentric and eccentric bracing systems in low, medium and high-rise buildings. The plastic mechanism for each system has also been modeled and the efficiencies and deficiencies of each have been discussed through various numerical examples. The effect of yields mechanisms and ductility demand patterns for various building types on the equivalent SDOF parameters have been investigated compared to the time history analysis results to find the sensitive parameters. Using the capacity design criteria, which leads to a known plastic mechanism, a simple procedure has also been obtained as an alternative approach for Push Over Analysis with much less computer time and effort.

Keywords

Displacement Based Design, Yield Mechanism, Ductility Demand Distribution, Braced Steel Buildings.

Introduction

In the Performance Based Design the structure is designed with sufficient and proportioned stiffness and strength in the structural members so as to develop inelastic action in the ductile designed members and to have appropriate over strength in the brittle members. Then the structure must be checked so that the demands do not exceed the existing capacities. This is best performed using a set of nonlinear dynamic analyses under earthquake with appropriate characters. Different design methods have been proposed based on performance criteria such as, Capacity Spectrum Method [1,2,3], N2 Method [4,5], Energy Based Methods and Displacement Based Design (DBD) Methods.

The idea of DBD has been introduced and developed by different researchers started by introducing the concept of substitute structure [6] in the last four decades. This idea has been adopted for a direct displacement design of SDOF and MDOF reinforced concrete bridges [7,8,9]. Capacity Spectrum Method and the N2 Method have also been used to create other direct DBD procedures [1,2,3,4,9,10]. In all of these researches, seismic demand is specified as either a displacement spectrum or an acceleration-displacement response spectrum. Generally nonlinear inelastic behaviour of a structural system can be accounted for either by an equivalent elastic response spectrum or an inelastic response spectrum. The former is